

On the Asymptotic Behavior of Ultra-Densification under a Bounded Dual-Slope Path Loss Model

Yanpeng Yang*, Jihong Park[†] and Ki Won Sung*

*KTH Royal Institute of Technology, Wireless@KTH, Stockholm, Sweden

E-mail: yanpeng@kth.se, sungkw@kth.se

[†]Dept. of Electronic Systems, Aalborg University, Denmark

Email: jihong@es.aau.dk

Abstract—In this paper, we investigate the impact of network densification on the performance in terms of downlink signal-to-interference (SIR) coverage probability and network area spectral efficiency (ASE). A sophisticated bounded dual-slope path loss model and practical UE densities are incorporated in the analysis. By using stochastic geometry, we derive an integral expression along with closed-form bounds of the coverage probability and ASE, validated by simulation results. Through these, we provide the asymptotic behavior of ultra-densification. The coverage probability and ASE have non-zero convergence in asymptotic regions unless UE density goes to infinity (full load). Meanwhile, the effect of UE density on the coverage probability is analyzed. The coverage probability will suffer from decreasing with large UE densities due to interference fall into the near-field, but it will keep increasing with lower UE densities. Furthermore, we show the performance is overestimated without applying the bounded dual-slope path loss model. Our study can give insights on efficient network provisioning in the future.

Index Terms—Network densification, bounded path loss model, dual-slope path loss model, stochastic geometry

I. INTRODUCTION

Network densification is considered as a key enabler to cope with the upcoming data tsunami for 5G [1] [2]. Deploying more base stations (BSs) can increase the network capacity rapidly by shortening the reuse distance and serving more user equipments (UEs) simultaneously. As densification goes on, BS density will exceed UE density, forming an ultra dense network (UDN) [3]. In this case, the network will transit from full load model to partial load model in which not all BSs are *active* (i.e., transmitting signals to serve the UEs within their cells), as shown in Fig. 1 from top to bottom. Such UDN may evaporate the advantage of densification since there is less than one UE per cell on average. Therefore, it is crucial to understand the asymptotic behavior of ultra densification for the purpose of efficient network deployment.

The preceding work [4] provides a comprehensive understanding on the impact of BS density in fully loaded downlink cellular networks with a simple single-slope path loss model. It concludes that BS densification does not change the signal-to-interference ratio (SIR) of an individual UE, but linearly improves the area spectral efficiency (ASE) defined as sum rate per unit area. However, this conclusion becomes inappropriate in a UDN due to its too simplified signal propagation and load models. In a UDN, BS-UE distance d shrinks, so a path loss model with a single exponent $\alpha > 2$ may

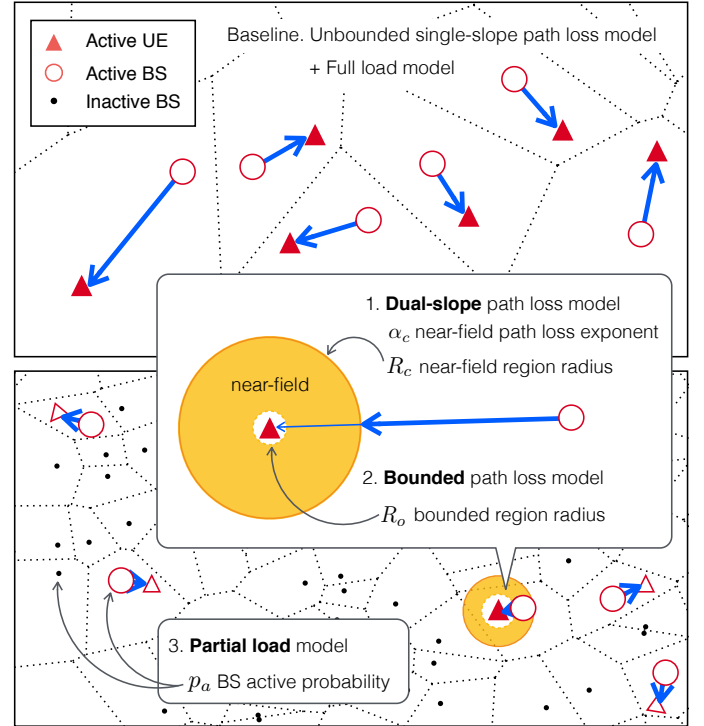


Fig. 1: Network layout of traditional fully loaded network (top) and partially loaded UDN (bottom) as well as illustration of the bounded dual-slope path loss model (middle).

amplify the received signal power $d^{-\alpha}$, which is unrealistic. In addition, a full load model where BSs always transmit signals overestimates interference although non-negligible portion of BSs in a UDN become inactive, not interfering with others. Thus, it is important to incorporate such propagation and load characteristics in detail in order to examine the impact of ultra densification.

To be precise, we consider that path loss attenuation from a BS to a UE is distinguished under two different regions, *near-field* and *far-field* at the UE as illustrated in Fig. 1. In a near-field within radius R_c , a transmitted signal experiences less absorption and diffraction, so the loss attenuation exponent α_c becomes less than α in the far-field, which leads to a *dual-slope* path loss model. In the innermost near-field, the

transmitted signal becomes no longer attenuated within radius R_o because of the physical volume of the UE, which leads to a *bounded* path loss model. The value of R_c is always no smaller than 1 so that the path loss model cannot amplify the transmitted signal power.

In addition, we consider a *partial load* model that incorporates not only active BSs but also inactive BSs as visualized at the bottom of Fig. 1. Under a nearest UE-BS association rule, each BS's active probability p_a is a monotonic decreasing function of BS density [5]. For sparse networks, p_a is close to 1, corresponding with a full load model where all the BSs interfere with others. For ultra-dense networks, p_a will decrease with BS density toward 0. This leads to interference decrease, yielding SIR improvement in UDNs [6], [7].

The effect of dual-slope model is investigated in [8], which concludes that UE coverage probability is a decreasing function of BS density. Meanwhile, [9] present the importance of applying bound in path loss models when BS density is extremely large. Both [8] and [9] provide vanishing SIR as BS density asymptotically grows. However, SIR increases toward infinity as BS density goes to infinity in [6] and [7]. Such contradiction comes from the corresponding models in the references. The bounded and dual-slope path loss models help to prevent overestimating the signal power and underestimating the interference respectively, which decrease the SIR. On the contrary, the partial load model can prevent overestimating the interference density in the whole network, which increases the SIR. Thus, a question emerges as: *what is the real asymptotic behavior of ultra densification?*

Motivated by the discussions, we aim to investigate the impact of network densification and its asymptotic behavior under a bounded dual-slope path loss model. To the best of our knowledge, this is the first work combining all the characteristics aforementioned: partial load model and a *bounded* plus *dual-slope* path loss model. The main contributions of this paper are listed below:

- Asymptotic convergence behaviors are present under a bounded dual-slope model in a partially loaded network. In asymptotic regions, both UE coverage probability and the ASE will converge to either zero or a constant (Prop. 3 and 4).
- Numerically tractable integral-form of coverage probability under a bounded dual-slope path loss model are derived (1). Moreover, closed-form bounds of coverage probability and ASE are provided (Prop. 2 and 4).
- The impact of UE density on coverage probability and ASE are analyzed (Fig. 2). Meanwhile, the trend of coverage probability and ASE are interpreted (Fig. 3 and Fig. 4). The scaling trend of ASE in terms of BS density is derived (Prop. 5).

II. SYSTEM MODEL

We consider a downlink cellular network where BSs and UEs are distributed according to two independent homogeneous Poisson Point Processes (PPPs) Φ_b and Φ_u . The densities of BS and UE are denoted as λ_b and λ_u respectively.

We assume each UE is associated with its closest BS whose coverage area comprises a Voronoi tessellation as shown in Fig. 1. Each BS becomes inactive without transmitting any signal when its coverage area, the Voronoi cell, is empty of active UEs. Correspondingly, each active BS has at least one UE in its cell and will randomly choose one of them to serve. The probability of a BS being active is derived in [5], given as:

$$p_a = 1 - (1 + \frac{\lambda_u}{3.5\lambda_b})^{-3.5}. \quad (1)$$

Both BS and UE are equipped with single antenna and BS transmits with unit power. Rayleigh fading is used to model the channel gain, with the fading coefficients h are i.i.d zero mean unit variance complex normal distributed random variables. Since we will focus on the asymptotic behavior and the system is interference-limited in dense networks, we will neglect the noise power and examine SIR throughout the paper.

We apply the bounded dual-slope path loss model introduced in the introduction part. The model can be formulated in a piece-wise function of the communication distance d , shown as

$$\ell(\alpha_1, \alpha_2, d) = \begin{cases} 1, & 0 \leq d \leq R_b; \\ d^{-\alpha_c}, & R_b < d \leq R_c; \\ \tau d^{-\alpha}, & d > R_c \end{cases} \quad (2)$$

where $R_b > 0$ is the radius of bounded path loss region, i.e., the path loss in the range of $[0, R_b]$ is assumed constant; $\tau \triangleq R_c^{\alpha - \alpha_c}$; $R_c \geq R_b$ is the critical distance to divide the near- and far-field; and α_c and α are the near- and far-field path loss exponents for $2 \leq \alpha_c \leq \alpha$, respectively.

A. Performance Metrics

In this paper, we will focus on two performance metrics from both user and network perspectives: SIR coverage probability of a typical UE and the ASE of the network. We analyze the performance of a typical user located at the origin o and randomly selected by the BS, which is permissible in a homogeneous PPP by Slivnyak's theorem [10]. The SIR of a typical user denoted as 0 can be expressed as

$$\text{SIR}_0 = \frac{|h_{0,0}|^2 \ell(d_{0,0})}{\sum_{i \in \Phi_b^* \setminus \{0\}} |h_{i,0}|^2 \ell(d_{i,0})}. \quad (3)$$

where $d_{i,j}$ and $h_{i,j}$ denote the distance and channel between BS i and UE j , $|h_{i,j}|^2 \sim \exp(1)$. Φ_b^* represents the set of active BSs which is not a homogeneous PPP. Nevertheless, we can assume Φ_b^* as a homogeneous PPP with density $\lambda_b^* = \lambda_b p_a$, which has been shown to be accurate according to [11] [12]. Given the downlink SIR of the typical user, the coverage probability is defined as:

$$P_c(\lambda_b, \lambda_u, T) \triangleq \mathbb{P}[\text{SIR}_0 > T] \quad (4)$$

where T is the target SIR level.

The network ASE Γ is defined as the sum average spectral efficiency of all active BSs achieving the target threshold in a unit area and is given by

$$\Gamma(\lambda_b, \lambda_u, T) \triangleq p_a \lambda_b P_c(\lambda_b, \lambda_u, T) \log_2(1 + T) \quad (5)$$

where $p_a \lambda_b P_c$ can be interpreted as the density of the BSs that successfully transmit the symbols to their users.

III. COVERAGE PROBABILITY AND ASE ANALYSIS

In this section, we derive the coverage probability and ASE expressions under a bounded dual-slope path loss model and provide closed-form bounds of them. Furthermore, we demonstrate the convergence of them in asymptotic regions where $\lambda_b \rightarrow \infty$.

Proposition 1: (Coverage probability expression) In a cellular network with BS active probability p_a , the coverage probability under a bounded dual-slope path loss model is expressed in (6) at the bottom of this page, where $F(b, z) = {}_2F_1(1, b, 1 + b, -z)$ with ${}_2F_1(a, b, c, z)$ being the Gauss hypergeometric function.

Proof: See Appendix A. ■

Despite the complicated form of (6), the first and third integrals can be calculated into exponential expressions. In this case, by applying transforms to the second integral, we can derive closed-form bounds of (6) with only exponential and hypergeometric functions as shown in the following proposition.

Proposition 2: (Coverage probability bounds) SIR coverage probability's lower bound P_c^{LB} and upper bound P_c^{UB} are given as (12) and (13) at the bottom of this page, where $H_1 = 1 - p_a \frac{T}{1+T}$, $H_{2l} = 1 + p_a G_2(R_b^2)$, $H_{2u} = 1 + p_a G_2(R_c^2)$, $H_3 = 1 + p_a G_3(T)$.

Proof: See Appendix B. ■

Applying Proposition 2 in asymptotic regions leads to the following proposition.

Proposition 3: (Asymptotic SIR coverage probability) As $\lambda_b \rightarrow \infty$, SIR coverage probability $P_c(\lambda_b, \lambda_u, T)$ converges to a finite value as follows.

$$\lim_{\lambda_b \rightarrow \infty} P_c(\lambda_b, \lambda_u, T) = e^{-\lambda_u \pi c_T(\alpha, \alpha_c, R_c, R_b)} \quad (12)$$

Proof: From (12) and (13) in Proposition 1, we have $\lim_{\lambda_b \rightarrow \infty} P_c^{\text{LB}} = \lim_{\lambda_b \rightarrow \infty} P_c^{\text{UB}} = \frac{1}{H_1} e^{-\lambda_u \pi c_T(\alpha, \alpha_c, R_c, R_b)}$ since all the other terms tend to 0 as $\lambda_b \rightarrow \infty$. According to the Squeeze theorem, $\lim_{\lambda_b \rightarrow \infty} P_c = \frac{1}{H_1} e^{-\lambda_u \pi c_T}$. Meanwhile, $\lim_{\lambda_b \rightarrow \infty} H_1 = 1$ since $p_a \rightarrow 0$. Thus $\lim_{\lambda_b \rightarrow \infty} P_c = e^{-\lambda_u \pi c_T(\alpha, \alpha_c, R_c, R_b)}$. ■

Proposition 3 emphasizes the importance of considering UE density in a UDN. The converged value is a decreasing function of λ_u and it tends to 0 when $\lambda_u \rightarrow \infty$, i.e., in a fully loaded network. Thus, deploying infinite number of BSs will not bring the UE performance to a unprecedented level. In contrast, extreme densification will put the coverage probability into the danger of decreasing to 0, as shown in Fig. 2 in the next section. The converged result also depends on environmental parameters $(\alpha, \alpha_c, R_c, R_b)$. It will increase as both path loss exponents grow since the coverage probability is a increasing function of path loss exponents [8]. A larger R_b or R_c will decline the performance since it either reduce the signal power or amplify the interference in the *near-field*.

We now turn to the network perspective and study the asymptotic behavior of the ASE. Combining the definition in (5) with Proposition 3, we can easily obtain the following proposition.

Proposition 4: (Asymptotic ASE) As $\lambda_b \rightarrow \infty$, ASE Γ converges to a finite value as follows.

$$\lim_{\lambda_b \rightarrow \infty} \Gamma(\lambda_b, \lambda_u, T) = \lambda_u e^{-\lambda_u \pi c_T(\alpha, \alpha_c, R_c, R_b)} \log_2(1 + T) \quad (13)$$

$$P_c(\lambda_b, \lambda_u, T) = \lambda_b \pi \left(\int_0^{R_b^2} e^{-\lambda_b \pi r(1+p_a G_1(r, T))} dr + \int_{R_b^2}^{R_c^2} e^{-\lambda_b \pi r(1+p_a G_2(r, T))} dr + \int_{R_c^2}^{\infty} e^{-\lambda_b \pi r(1+p_a G_3(T))} dr \right) \quad (6)$$

$$(7)$$

where

$$G_1(r, T) = c_T(\alpha, \alpha_c, R_c, R_b) r^{-1} - T(1 + T)^{-1} \quad (8)$$

$$G_2(r, T) = \left[c_T(\alpha, \alpha_c, R_c, \sqrt{r}) + R_b^2 \left(F\left(\frac{2}{\alpha}, \frac{1}{T}\right) - \frac{T}{1+T} \right) \right] r^{-1} - F\left(\frac{2}{\alpha}, T^{-1}\right) \quad (9)$$

$$G_3(T) = T \left(\frac{\alpha_c}{2} - 1 \right)^{-1} F\left(1 - \frac{2}{\alpha_c}, T\right) \quad (10)$$

$$c_T(\alpha, \alpha_c, R_c, x) := R_c^2 F\left(\frac{2}{\alpha}, \frac{1}{T} \left[\frac{R_c}{x} \right]^\alpha\right) - R_b^2 \left[F\left(\frac{2}{\alpha}, \frac{1}{T}\right) - \frac{T}{1+T} \right] + \frac{2TR_b^\alpha R_c^{2-\alpha}}{\alpha_c - 2} F\left(1 - \frac{2}{\alpha_c}, T \left[\frac{x}{R_c} \right]^\alpha\right) \quad (11)$$

$$P_c^{\text{LB}} = \frac{1}{H_1} \left(e^{-\lambda_b p_a \pi c_T(\alpha, \alpha_c, R_c, R_b)} - e^{-\lambda_b \pi (R_b^2 H_1 + p_a c_T(\alpha, \alpha_c, R_c, R_b))} \right) + \frac{1}{H_{2l}} \left(e^{-\lambda_b \pi R_b^2 H_{2l}} - e^{-\lambda_b \pi R_c^2 H_{2l}} \right) + \frac{1}{H_3} \left(e^{-\lambda_b \pi R_c^2 H_3} \right) \quad (12)$$

$$P_c^{\text{UB}} = \frac{1}{H_1} \left(e^{-\lambda_b p_a \pi c_T(\alpha, \alpha_c, R_c, R_b)} - e^{-\lambda_b \pi (R_b^2 H_1 + p_a c_T(\alpha, \alpha_c, R_c, R_b))} \right) + \frac{1}{H_{2u}} \left(e^{-\lambda_b \pi R_b^2 H_{2u}} - e^{-\lambda_b \pi R_c^2 H_{2u}} \right) + \frac{1}{H_3} \left(e^{-\lambda_b \pi R_c^2 H_3} \right) \quad (13)$$

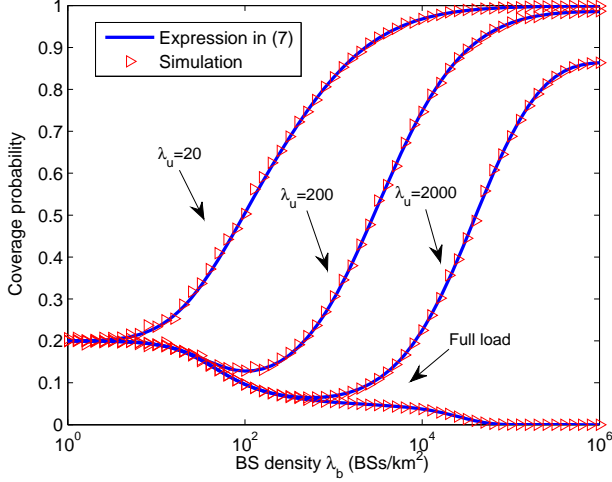


Fig. 2: Effect of λ_u on coverage probability under bounded dual-slope model.

Proposition 4 shows that the asymptotic ASE will increase with λ_u when λ_u is small and tends to 0 as $\lambda_u \rightarrow \infty$. Unlike the coverage probability, the asymptotic ASE will be beneficial from ultra-desification to some extent and but still highly depends on the UE density.

Returning from the asymptotic regions, we demonstrate how the ASE scales with BS density in the next proposition.

Proposition 5: (ASE scaling) The ASE scales with $\lambda_b p_a e^{-\lambda_b p_a \pi c_T (\alpha, \alpha_c, R_c, R_b)}$ and is bounded by

$$\Gamma^{\text{LB}} = \lambda_b p_a P_c^{\text{LB}} \log_2(1 + T) \quad (14)$$

$$\Gamma^{\text{UB}} = \lambda_b p_a P_c^{\text{UB}} \log_2(1 + T). \quad (15)$$

Proof: See Appendix C. ■

Similar with its asymptotic behavior, the ASE will increase with BS density when λ_b is small and finally converge to $\lambda_u e^{-\lambda_u \pi c_T} \log_2(1 + T)$ as shown in Proposition 4.

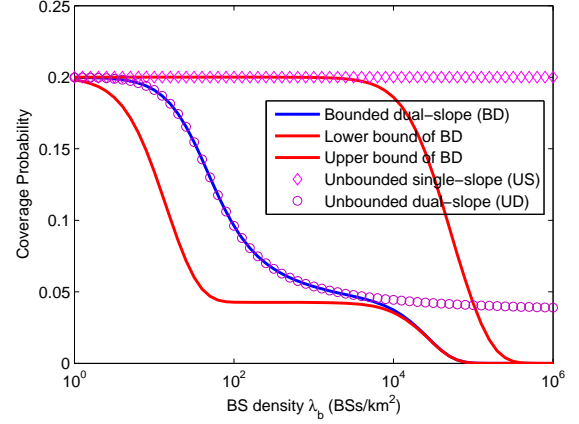
IV. NUMERICAL RESULTS

In this section, we present the numerical results to study the performance of network densification and validate our theoretical analysis. We assume $R_b = 1m$, $R_c = 70m$, $\alpha_c = 2.5$, $\alpha = 4$ and set the SIR threshold $T = 10\text{dB}$ in all of our results. To calculate or simulate ‘fully loaded network’, we set $\lambda_u = 2 \times 10^8/\text{km}^2$ which is a sufficiently large value so that $p_a \approx 1$.

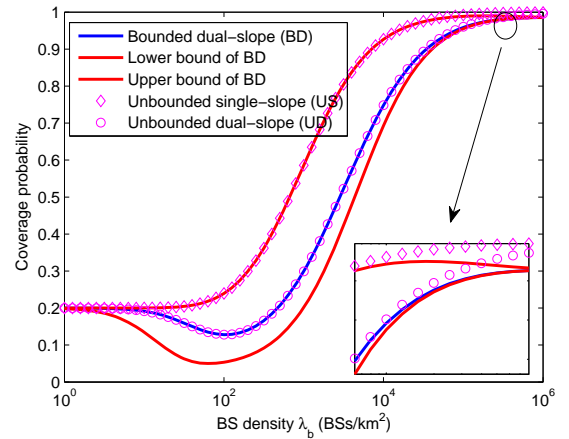
A. Effect of UE density

Fig. 2 shows the effect of UE density on coverage probability. An exact match between simulation and analysis is observed. Meanwhile, we find that coverage probabilities show completely different trends among different UE densities.

In full load model, the diminishing of coverage probability starts when interfering BSs fall into the *near-field* of the



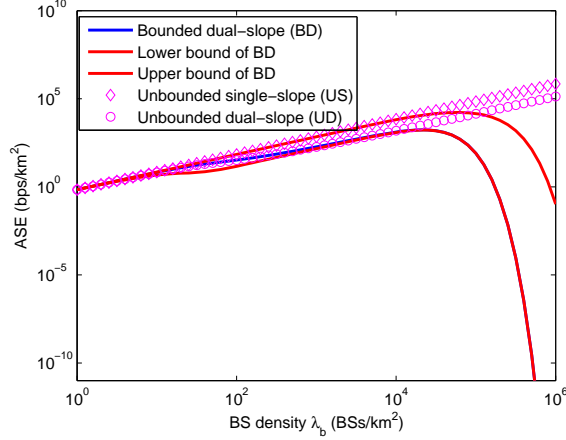
(a) Coverage Probability when network is fully loaded



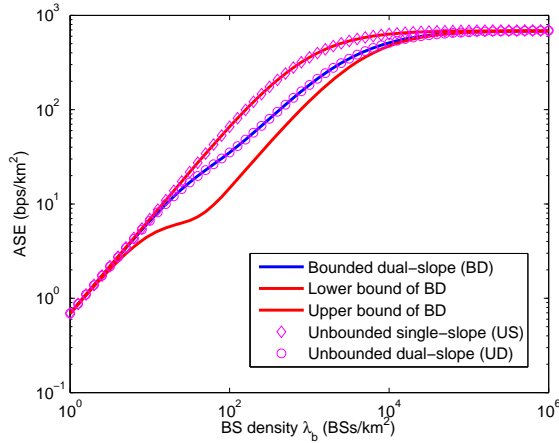
(b) Coverage Probability when $\lambda_u = 200$

Fig. 3: Coverage probability bounds and comparison with previous models

typical UE and keeps decreasing since interference will continue increasing. When λ_u is finite, the interferer coordinates converge to UE coordinates in a UDN regime [6]. Thus the distance from the typical UE to its closest interferer can be approximated as the distance to its closest neighbor UE, which has an expected value of $\frac{1}{2\sqrt{\lambda_u}}$. When UE density is low (e.g. $\lambda_u = 20$), the expected value is larger than the critical distance, which means the probability of no interferer inside the *near-field* of the typical UE is very high. Hence, the coverage probability is a non-decreasing function of λ_b as in a single-slope model. In contrast, higher UE density (e.g. $\lambda_u = 200$ or 2000) leads to more potential interferers within critical distance. Thus coverage probability will decrease for the same reason as in fully loaded network. Nevertheless, when all the UEs in the *near-field* get service, coverage probability will start increasing again since the interference is saturated and no longer increase. Therefore, it is important to estimate the active UE density for efficient network deployment or operation in order to avoid the decreasing region of coverage probability.



(a) ASE when network is fully loaded



(b) ASE when $\lambda_u = 200$

Fig. 4: ASE bounds and comparison with previous models.

B. Coverage probability analysis

In Fig. 3, we compare the coverage probability under our model with the previous models. We observe that the performance is overestimated with unbounded or single-slope models in highly densified regions. The reason is that those models either exaggerate the received power inside the bounded region or underestimate the interference in the near-field.

The inaccuracy of path loss models may mislead the prediction of asymptotic behavior. For instance, the coverage probability will converge to 1 with unbounded models but to $e^{-\lambda_u \pi c_T(\alpha, \alpha_c, R_c, R_b)}$ which is smaller than 1 (assume $\lambda_u > 0$) when applying a bounded model. Consistent with the result in Proposition 3, the converged value will decrease as UE density grows and finally falls to zero in the full load case as shown in Fig. 2. This is because the signal is limited by the bound effect and the overall performance will be dominated by the interference which depends on UE density.

C. ASE analysis

Figure 4 depicts the scaling of ASE with regard to BS density. Aligning with proposition 5, the ASE first increase

with BS density and then converge to a constant. The constant is larger than 0 in partially loaded network and decreases to 0 when the network is full load ($\lambda_u \rightarrow \infty$) as proved in Proposition 4.

By comparing Fig. 4 with Fig. 3, we can observe a trade-off between UE and network performance during BS densification. In full load case, there exists an BS density threshold around $\lambda_b = 10^4$. Before the threshold, although individual performance gets worse, densification is still beneficial from the network perspective. For partially loaded network, the trade-off appears approximately between $\lambda_b = 10^{1.5}$ to $\lambda_b = 10^3$. The phenomenon further demonstrates the necessity of applying a dual-slope model because the coverage probability is a non-decreasing function of BS density in a single-slope model.

Our bounds in Proposition 2 and 5 are compared with the integral expression and shown in Fig. 3 and 4. The figures verify the asymptotic tightness of the bounds for $\lambda \rightarrow \infty$. The upper bound is tighter in small UE density scenarios while the lower bound fits better for large UE densities. This is because the upper bound is close to single-slope model which is similar with small UE density scenario. The bounds can be used as approximations in large BS density regions.

V. CONCLUSION AND FUTURE WORK

In this paper, we investigate the asymptotic behavior of ultra-densification of base stations. To our best knowledge, this is the first work incorporating two key aspects of UDN modeling: a partially loaded network due to finite UE density and a dual-slope path loss model with a bounded loss within a unit distance. With such models, we find that the asymptotic behavior of ultra-dense base station deployment is different from what was known with simpler assumptions. Depending on the UE density, both UE coverage probability and ASE converge to either zero or a constant value. Our results also suggest that the densification cannot always improve the individual UE performance or boost the network throughput. Our work provides insights into the scaling of the network densification, and thus gives a guideline for the network deployment.

APPENDIX A PROOF OF PROPOSITION 1

We start from the coverage probability expression under general path loss model and then plug in with our bounded dual-slope model. According to the definition, the coverage probability can be expressed as:

$$\begin{aligned}
 P_c^l &= \mathbb{P}[\text{SIR} > T] = \mathbb{P}\left[\frac{|h|^2 \ell(r)}{I} > T\right] \\
 &\stackrel{(a)}{=} \int_{r>0} \mathbb{P}\left[|h|^2 > \frac{TI}{\ell(r)} \mid r\right] f_r(r) dr \\
 &\stackrel{(b)}{=} \int_{r>0} \mathcal{L}_I\left(\frac{T}{\ell(r)}\right) f_r(r) dr
 \end{aligned} \tag{16}$$

where (a) follows from BS distribution and (b) is due to the fact that $|h|^2 \sim \exp(1)$, $\mathcal{L}_I(s)$ is the Laplace transform of interference which can be derived as

$$\begin{aligned}\mathcal{L}_I(s) &= \mathbb{E}_I[e^{-sI}] = \mathbb{E}_{\Phi_b^*, g_i}[\exp(-s(\sum_{x \in \Phi_b^*} g_i \ell(d_i)))] \\ &\stackrel{(a)}{=} \mathbb{E}_{\Phi_b^*} \left[\prod_{x \in \Phi_b^*} \frac{1}{1 + s\ell(d_i)} \right] \\ &\stackrel{(b)}{=} \exp \left(-2\pi\lambda_b^* \int_r^\infty \left(1 - \frac{1}{1 + s\ell(v)} \right) dv \right)\end{aligned}\quad (17)$$

where (a) is because $g \sim \exp(1)$ and (b) follows the probability generating functional (PGFL) of the PPP. Plugging in $s = \left(\frac{T}{\ell(r)}\right)$ and employing a change of variables $v = \sqrt{tr}$ results in

$$\mathcal{L}_I\left(\frac{T}{\ell(r)}\right) = \exp \left(-2\pi\lambda_b P_a \int_1^\infty \left(\frac{T}{T + \frac{\ell(r)}{\ell(\sqrt{tz})}} \right) dt \right). \quad (18)$$

Plugging (18) into (16) with $z \rightarrow r^2$ gives the coverage probability under a general path loss function in (19) as:

$$P_c^I(\lambda_b, \lambda_u, T) = \lambda_b \pi \int_0^\infty \exp \left(-\lambda_b \pi z \left[1 + p_a \int_1^\infty \frac{1}{1 + \frac{\ell(\sqrt{z})}{T\ell(\sqrt{tz})}} dt \right] \right) dz \quad (19)$$

Based on (19), we can substitute our bounded dual-slope model (2) into it and get the expression in (6).

APPENDIX B

PROOF OF PROPOSITION 2

According to the expression of (8) and (10), $rG_1(r, T)$ and $rG_3(T)$ are linear functions of r . Thus we can rewrite the first and third integral in (6) as follows:

$$\int_0^{R_b^2} e^{-\lambda_b \pi r(1+p_a G_1(r))} dr = \frac{1}{H_1} \left(e^{-\lambda_b p_a \pi c_T} - e^{-\lambda_b \pi (R_b^2 H_1 + p_a c_T)} \right) \quad (20)$$

$$\int_{R_c^2}^\infty e^{-\lambda_b \pi r(1+p_a G_3(r))} dr = \frac{1}{H_3} \left(e^{-\lambda_b \pi R_c^2 H_3} \right). \quad (21)$$

In the second integral, from $G_2'(r) < 0$ we can get $G_2(R_b^2) \geq G(r) \geq G_2(R_c^2)$. With the inequality, we can provide bounds for the second integral as:

$$\begin{aligned}\int_{R_b^2}^{R_c^2} e^{-\lambda_b \pi r(1+p_a G_2(r))} dr &\leq \int_{R_b^2}^{R_c^2} e^{-\lambda_b \pi r(1+p_a G_2(R_b^2))} dr \\ &= \frac{1}{H_{2u}} (e^{-\lambda_b \pi H_{2u} R_b^2} - e^{-\lambda_b \pi H_{2u} R_c^2})\end{aligned}\quad (22)$$

$$\begin{aligned}\int_{R_b^2}^{R_c^2} e^{-\lambda_b \pi r(1+p_a G_2(r))} dr &\geq \int_{R_b^2}^{R_c^2} e^{-\lambda_b \pi r(1+p_a G_2(R_c^2))} dr \\ &= \frac{1}{H_{2l}} (e^{-\lambda_b \pi H_{2l} R_b^2} - e^{-\lambda_b \pi H_{2l} R_c^2}).\end{aligned}\quad (23)$$

Replacing the integrals in (6) with the exponential expressions above completes the proof.

APPENDIX C

PROOF OF PROPOSITION 3

Notation: Let f and g be two functions defined on some subset of the real numbers. One writes $f(x) = \mathcal{O}(g(x))$ if and only if there exists a positive real number M and a real number x_0 such that $f(x) \leq Mg(x)$ for all $x \geq x_0$.

We omit the proof of the bounds since they come directly from Proposition 2. To prove the ASE scales with $\lambda_b^* e^{-\lambda_b^* \pi c_T}$ is equivalent with showing $\Gamma^{\text{UB}} = \mathcal{O}(\lambda_b^* e^{-\lambda_b^* \pi c_T})$ and $\lambda_b^* e^{-\lambda_b^* \pi c_T} = \mathcal{O}(\Gamma^{\text{LB}})$. Denote $\log_2(1+T)$ as τ and from (13) we have:

$$\Gamma^{\text{UB}} \leq \lambda_b^* \left(\frac{1}{H_1} e^{-\lambda_b p_a \pi c_T} + \frac{1}{H_{2u}} e^{-\lambda_b \pi H_{2u} R_b^2} + \frac{1}{H_3} e^{-\lambda_b \pi H_3 R_c^2} \right) \tau. \quad (24)$$

Then we can show $\exists \lambda_1 > 0, \forall \lambda_b > \lambda_1, \frac{1}{H_1} e^{-\lambda_b p_a \pi c_T} > \frac{1}{H_{2u}} e^{-\lambda_b \pi H_{2u} R_b^2}$ and $\frac{1}{H_1} e^{-\lambda_b p_a \pi c_T} > \frac{1}{H_3} e^{-\lambda_b \pi H_3 R_c^2}$ since $\frac{1}{H_1} e^{-\lambda_b p_a \pi c_T} \rightarrow \frac{1}{H_1} e^{-\lambda_u \pi c_T}$ and the other two parts $\rightarrow 0$ as $\lambda_b \rightarrow \infty$. Thus $\exists \lambda_1 > 0, \forall \lambda_b > \lambda_1, \Gamma^{\text{UB}} \leq \frac{3}{H_1} \lambda_b^* e^{-\lambda_b^* \pi c_T} \Rightarrow \Gamma^{\text{UB}} = \mathcal{O}(\lambda_b^* e^{-\lambda_b^* \pi c_T})$.

For Γ^{LB} , from (12) we have

$$\Gamma^{\text{LB}} \geq \frac{1}{k_1} \lambda_b^* \left(e^{-\lambda_b p_a \pi c_T} - e^{-\lambda_b \pi (H_1 R_b^2 + p_a c_T)} \right) \tau, \quad (25)$$

which can be rephrased as:

$$\lambda_b^* e^{-\lambda_b p_a \pi c_T} \leq \frac{H_1}{(1 - e^{-\lambda_b \pi H_1 R_b^2}) \tau} \Gamma^{\text{LB}}. \quad (26)$$

Thus, $\exists \lambda_2 > 0, k > 0, \forall \lambda_b > \lambda_2, e^{-\lambda_b \pi H_1 R_b^2} < k$ thus $\lambda_b^* e^{-\lambda_b p_a \pi c_T} \leq \frac{H_1}{(1-k)\tau} \Gamma^{\text{LB}}$. Therefore $\lambda_b^* e^{-\lambda_b^* \pi c_T} = \mathcal{O}(\Gamma^{\text{LB}})$ and we complete the proof.

REFERENCES

- [1] N. Bhushan, J. Li, D. Malladi, R. Gilmore, D. Brenner, A. Damnjanovic, R. T. Sukhvasi, C. Patel, and S. Geirhofer, "Network densification: the dominant theme for wireless evolution into 5g," *IEEE Communications Magazine*, vol. 52, no. 2, pp. 82–89, February 2014.
- [2] M. Kamel, W. Hamouda, and A. Youssef, "Ultra-dense networks: A survey," *IEEE Communications Surveys Tutorials*, vol. PP, no. 99, pp. 1–1, 2016.
- [3] D. López-Pérez, M. Ding, H. Claussen, and A. H. Jafari, "Towards 1 gbps/ue in cellular systems: Understanding ultra-dense small cell deployments," *IEEE Communications Surveys Tutorials*, vol. 17, no. 4, pp. 2078–2101, Fourthquarter 2015.
- [4] J. Andrews, F. Baccelli, and R. Ganti, "A tractable approach to coverage and rate in cellular networks," *Communications, IEEE Transactions on*, vol. 59, no. 11, pp. 3122–3134, November 2011.
- [5] S. M. Yu and S.-L. Kim, "Downlink capacity and base station density in cellular networks," in *Modeling Optimization in Mobile, Ad Hoc Wireless Networks (WiOpt)*, 2013 11th International Symposium on, May 2013, pp. 119–124.
- [6] J. Park, S. L. Kim, and J. Zander, "Asymptotic behavior of ultra-dense cellular networks and its economic impact," in *2014 IEEE Global Communications Conference*, Dec 2014, pp. 4941–4946.
- [7] Y. Yang and K. W. Sung, "Tradeoff between spectrum and densification for achieving target user throughput," in *2015 IEEE 81st Vehicular Technology Conference (VTC Spring)*, May 2015, pp. 1–6.
- [8] X. Zhang and J. G. Andrews, "Downlink cellular network analysis with multi-slope path loss models," *IEEE Transactions on Communications*, vol. 63, no. 5, pp. 1881–1894, May 2015.
- [9] J. Liu, M. Sheng, L. Liu, and J. Li, "Effect of densification on cellular network performance with bounded pathloss model," *IEEE Communications Letters*, vol. PP, no. 99, pp. 1–1, 2016.
- [10] D. Stoyan, W. Kendall, and J. Mecke, *Stochastic Geometry and Its Applications*. John Wiley and Sons, 1996.

- [11] S. Lee and K. Huang, "Coverage and economy of cellular networks with many base stations," *Communications Letters, IEEE*, vol. 16, no. 7, pp. 1038–1040, July 2012.
- [12] C. Li, J. Zhang, and K. Letaief, "Throughput and energy efficiency analysis of small cell networks with multi-antenna base stations," *Wireless Communications, IEEE Transactions on*, vol. 13, no. 5, pp. 2505–2517, May 2014.